



2 Studying the vertical variation of cloud droplet effective radius using 3 ship and space-borne remote sensing data

4 Ruiyue Chen,^{1,2} Robert Wood,³ Zhanqing Li,^{1,2} Ralph Ferraro,^{2,4} and Fu-Lung Chang,⁵

5 Received 12 November 2007; revised 28 February 2008; accepted 2 May 2008; published XX Month 2008.

6 [1] The albedo of marine stratocumuli depends upon cloud liquid water content, droplet
7 effective radius (r_e), and how these parameters vary with height. Using satellite data
8 and shipborne data from the East Pacific Investigation of Climate (EPIC) Stratocumulus
9 Study, this study investigates the cloud r_e vertical variation for drizzling and nondrizzling
10 clouds. Visible/near-infrared retrievals from the NASA Moderate Resolution Imaging
11 Spectroradiometer (MODIS) are used to estimate the vertical profile of r_e . MODIS r_e
12 observations and collocated shipborne scanning C-band precipitation radar data show that
13 r_e generally increases with height in nondrizzling clouds, consistent with aircraft
14 observations. It is found that in clouds with precipitation rates greater than a few
15 hundredths of a mm h^{-1} the vertical gradient of r_e is significantly less than that in
16 nondrizzling clouds and can become negative when the drizzle is heavier than
17 approximately 0.1 mm h^{-1} . High values of r_e at drizzling cloud base are consistent with
18 estimates of the ratio of liquid water in the drizzle drops to that in the cloud droplets.
19 C-band derived cloud base precipitation rates are found to be better correlated with r_e at
20 cloud base than with r_e at cloud top, suggesting that passive remote sensing may be useful
21 for drizzle detection.

22 **Citation:** Chen, R., R. Wood, Z. Li, R. Ferraro, and F.-L. Chang (2008), Studying the vertical variation of cloud droplet effective
23 radius using ship and space-borne remote sensing data, *J. Geophys. Res.*, 113, XXXXXX, doi:10.1029/2007JD009596.

25 1. Introduction

26 [2] Low-level stratiform liquid water clouds have a significant influence on the Earth's climate due to their strong
27 shortwave radiative forcing [Greenwald *et al.*, 1995]. Such clouds cover large regions of the Earth's oceans [Klein and
28 Hartmann, 1993]. The shortwave optical depth of liquid
29 water clouds depends upon both the bulk condensate
30 amount and the size of the cloud drops. Dependence on
31 the latter is conveniently expressed as an effective radius
32 which is the ratio of the third to second moments of the
33 cloud droplet size distribution.

34 [3] The vertical variation of cloud droplet effective radius
35 (r_e) is an important cloud property which reflects both
36 condensation and coalescence growth. There are different
37 ways to obtain information on the vertical profile of cloud
38 r_e , including in situ aircraft measurements [e.g., Martin *et*
39 *al.*, 1994; Wood, 2000; Miles *et al.*, 2000] and new retrievals
40 from satellite measurements of solar reflectance [Chang and
41 Li, 2002].

42 The aircraft measurements in low clouds show 43
44 that r_e generally increases with height for nondrizzling 44
45 clouds [Martin *et al.*, 1994; Miles *et al.*, 2000; Wood, 45
46 2000] but that drizzle drops start to increase the effective 46
47 radius significantly if the liquid water content of drizzle 47
48 drops is above 5–10% of the liquid water content of small 48
49 cloud droplets [Wood, 2000]. These drizzle droplets thus 49
50 reduce the vertical gradient and even lead to r_e decreasing 50
51 with height because drizzle drops tend to increase in size 51
52 toward the base of the cloud [Wood, 2005a]. However, only 52
53 limited work has been carried out to examine the vertical 53
54 profile of effective radius in drizzling low clouds. Drizzle 54
55 commonly occurs in marine low clouds and its effects upon 55
56 cloud optical properties are very poorly understood 56
57 [Albrecht, 1989; Wood, 2005a; Comstock *et al.*, 2004; 57
58 VanZanten *et al.*, 2005].

59 [4] Satellite observation is the only practical way to infer 59
60 cloud r_e globally. Solar reflectance measurements from a 60
61 visible channel and a near infrared (NIR) channel are widely 61
62 used to estimate cloud optical depth and cloud top r_e 62
63 [Nakajima and King, 1990; Han *et al.*, 1994]. Using radar 63
64 and a solar/infrared radiometer on board the Tropical 64
65 Rainfall Measuring Mission (TRMM), Kobayashi [2007] 65
66 found that cloud r_e of precipitating clouds is obviously 66
67 larger than that for nonprecipitating clouds. In previous 67
68 studies, cloud r_e retrievals have used three NIR channels, 68
69 which have wavelengths of $\lambda = 1.6 \mu\text{m}$, $2.1 \mu\text{m}$, and $3.7 \mu\text{m}$ 69
70 [King *et al.*, 2003]. Because clouds absorption is different at 70
71 the three wavelengths, the NIR channels have different 71
72 reflectance weighting functions from cloud top to cloud 72

¹Department of Atmospheric and Oceanic Sciences, University of Maryland, College Park, Maryland, USA.

²Cooperative Institute for Climate Studies, University of Maryland, College Park, Maryland, USA.

³Department of Atmospheric Sciences, University of Washington, Seattle, Washington, USA.

⁴Center for Satellite Applications and Research, NESDIS, NOAA, Camp Springs, Maryland, USA.

⁵National Institute for Aerospace, Hampton, Virginia, USA.

73 base. *Platnick* [2000] found the weighting function for $\lambda =$
 74 $3.7 \mu\text{m}$ is mainly confined to the cloud top layer (i.e., within
 75 optical depth 2) and sharply decrease toward cloud base,
 76 while the weighting function at $\lambda = 1.6 \mu\text{m}$ spreads more
 77 evenly into the lower cloud layer (i.e., for a cloud with
 78 optical depth equal to 8, the weighting function value at
 79 cloud base is around half of its maximum value). Conse-
 80 quently, the $\lambda = 3.7 \mu\text{m}$ retrieval corresponds to the r_e close
 81 to the top of the cloud layer, whereas the $\lambda = 2.1 \mu\text{m}$ and
 82 $\lambda = 1.6 \mu\text{m}$ retrievals are sensitive to r_e values deeper
 83 inside the cloud. Assuming that the r_e has a linear distribu-
 84 tion in the vertical direction, *Chang and Li* [2002, 2003,
 85 hereinafter referred to as CL] present a method to determine
 86 an optimal linear r_e profile by using a combination of NIR
 87 measurements at $\lambda = 3.7 \mu\text{m}$, $2.1 \mu\text{m}$, and $1.6 \mu\text{m}$. The linear
 88 r_e assumption is based on many r_e profile measurements
 89 worldwide [*Miles et al.*, 2000; *Wood*, 2000; *Brenguier et al.*,
 90 2000].

91 [5] Applying the CL algorithm to reflectance measure-
 92 ments from the Moderate Resolution Imaging Spectroradi-
 93 ometer (MODIS) on the NASA Aqua satellite, *Chen et al.*
 94 [2007] conducted a preliminary study to show that the
 95 distributions of r_e profile are different for drizzling and
 96 nondrizzling clouds. However, the definition of drizzling
 97 used in their study was based on an empirical threshold of
 98 liquid water path (LWP), which is retrieved from brightness
 99 temperature measurements from the Advanced Microwave
 100 Scanning Radiometer (AMSR-E) on Aqua. The threshold-
 101 based detection of drizzling suffers from an ambiguity
 102 caused by cloud LWP (i.e., it is not clear how to separate
 103 the detected LWP into cloud and rain components) and has
 104 difficulty detecting light drizzle [*Zuidema et al.*, 2005].
 105 Failure to detect light drizzle could also be caused by the
 106 nearly 100 km^2 field of view size of AMSR-E 37 GHz
 107 channel, which is the primary channel used in LWP esti-
 108 mation [*Ashcroft and Wentz*, 2000].

109 [6] In this study, measurements from the East Pacific
 110 Investigation of Climate (EPIC) Stratocumulus Study are
 111 used for cloud profile analysis. Coincident radiance mea-
 112 surements from MODIS on the Terra satellite are used to
 113 estimate the r_e profile with the CL algorithm. Through a
 114 synergistic analysis of radar reflectivity profile measured by
 115 a millimeter cloud radar (MMCR), drizzle measurements
 116 from a scanning C-band radar, and satellite estimation of the
 117 (assumed linear) r_e profile, the vertical variation of cloud r_e
 118 is estimated for both drizzling and nondrizzling clouds.
 119 Such analysis was not possible in previous studies because
 120 of the lack of observation of cloud r_e profile and drizzle.
 121 The estimation of vertical r_e variation and how it depends
 122 upon the drizzle rate provide useful information for drizzle
 123 detection, cloud modeling, and climate studies (i.e., study of
 124 aerosol indirect effect).

125 [7] Section 2 introduces the instruments that are used in
 126 this study and the data processing methods. The uncertain-
 127 ties of the data from these instruments are also discussed. In
 128 section 3, estimates of the partitioning of liquid water
 129 content between drizzle drops and small cloud droplets is
 130 carried out using MMCR data in drizzling stratocumulus by
 131 incorporating simultaneous LWP estimates from a passive
 132 microwave radiometer. Drizzle precipitation rates obtained
 133 from the C-band radar and spatiotemporally matched r_e
 134 profile estimation from MODIS satellite measurements are

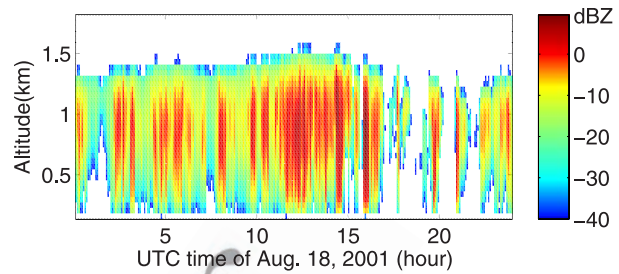


Figure 1. Millimeter cloud radar reflectivity measurements on 18 October 2001.

combined to evaluate the impact of drizzle on the trend of 135
 vertical r_e variation. Section 4 summarizes the result of this 136
 study, discusses the potential of profile retrieval on drizzle 137
 detection, and presents further research need to be done in 138
 the future. 139

2. Data and Methods 140

[8] The EPIC Stratocumulus Study [*Bretherton et al.*, 141
 2004] was conducted in October 2001 within the southeast- 142
 ern Pacific stratocumulus region. From 16 to 22 October, 143
 the NOAA research vessel R/V *Ronald Brown* (RHB) was 144
 stationary at 20°S , 85°W and observed a relatively well- 145
 mixed boundary layer with predominantly overcast skies 146
 and few upper level clouds. Comprehensive cloud and 147
 precipitation measurements were taken by vertically point- 148
 ing remote sensing instruments on the RHB. This investi- 149
 gation uses cloud profile and drizzle estimates at 20°S , 150
 85°W from EPIC instruments, as well as r_e profile estima- 151
 tion from spatiotemporally matched data from MODIS on 152
 Terra. 153

2.1. Cloud Measurements From Millimeter Radar, 154 Ceilometer, and Microwave Radiometer 155

[9] Cloud reflectivity profiles are provided by vertically 156
 pointing 8.6mm wavelength radar (MMCR), which has a 157
 vertical resolution of 45 m [*Moran et al.*, 1998]. The beam 158
 width is 0.5° and the minimum detectable reflectivity is 159
 around -60 dBZ . The radar obtains a reflectivity profile 160
 every 10 s, but the reflectivity profile measurements are 161
 averaged to a 5 min temporal resolution for this study 162
 (equivalent to approximately 5 km horizontal spatial res- 163
 olution). The calibration error of MMCR data are less than 164
 1 dBZ . *Comstock et al.* [2004] showed that the uncertainty 165
 of the MMCR radar measurements caused by Mie scattering 166
 is less than 10% for stratocumulus clouds given the mean 167
 radii of cloud and drizzle drops encountered in EPIC. Cloud 168
 top height is determined using a reflectivity threshold of 169
 -40 dBZ to define cloud, a value that leads to cloud top 170
 heights very close to the height of the inversion base as 171
 determined using radiosondes (not shown). The cloud base 172
 height is measured using a ceilometer with 15 m vertical 173
 resolution. The LWP is estimated from brightness temper- 174
 ature measurements of a microwave radiometer at 22 GHz 175
 and 31 GHz [*Zuidema et al.*, 2005]. The uncertainty of 176
 the LWP estimation is around $10\text{--}25 \text{ g}^{-2}$. Figure 1 shows 177
 an example of MMCR reflectivity measurements for a 24 h 178
 period (18 October 2001) in which significant drizzle was 179
 observed to fall [see *Comstock et al.*, 2004]. In this study, 180

181 estimates of the partitioning of liquid water content between
182 drizzle drops and small cloud droplets is carried out using
183 MMCR data in stratocumulus by incorporating simulta-
184 neous LWP estimates from a passive microwave radiometer.

185 2.2. Estimates of Drizzle From Scanning C-Band 186 Radar

187 [10] The C-band radar on the RHB has a 5 cm wavelength
188 and 0.95° beam width. During EPIC, the C-band completed
189 an 11-elevation angle volumetric scan out to 30 km radius
190 every 5 min [Comstock *et al.*, 2004]. Reflectivity between
191 0.5 km and 2 km altitude is averaged to produce two-
192 dimensional maps with an estimated calibration error of
193 ± 2.5 dBZ. The minimum detectable reflectivity is approx-
194 imately -12 dBZ at 30 km distance. Because of its
195 sensitivity, C-band measurements in low water clouds are
196 only sensitive to drizzle, as cloud liquid water content
197 cannot produce the reflectivity at sufficient magnitude to
198 be detected. In this study, the cloud base precipitation rate is
199 estimated using $Z = 25R^{1.3}$, where Z is the radar reflectivity
200 in mm^6m^{-3} , and R is the rain rate in mm h^{-1} . This $Z - R$
201 relationship was derived using vertically pointing MMCR
202 data in drizzling stratocumulus during EPIC [Comstock *et al.*,
203 2004] and consistent with aircraft in situ measurements
204 in drizzling stratocumulus [Wood, 2005b]. The C-band
205 measurements are compared with the r_e profile retrieval
206 from MODIS on Terra described below.

207 2.3. Cloud Profile Retrieval Using MODIS

208 [11] MODIS L1B reflectance measurements at $\lambda = 0.86$
209 μm , $1.6 \mu\text{m}$, $2.1 \mu\text{m}$, and $3.7 \mu\text{m}$ from Terra satellite are
210 used to estimate cloud optical depth, the r_e profile, and the
211 LWP using the CL algorithm at a nadir resolution of 1×1
212 km^2 . Only daytime MODIS measurements are used in this
213 study because solar reflectance measurements are needed
214 for retrieving cloud parameters. The Terra overpass time is
215 close to 1600 UTC at 20°S , 85°W , when the solar zenith
216 angle is between 20° and 30° during October. The satellite
217 zenith angle of MODIS ranges between -55° and 55° .

218 [12] In the CL algorithm, the linear r_e profile is defined as
219 a function of height z , which is defined by

$$r_e(z') = r_{e1} + (r_{e2} - r_{e1})z', \quad (1)$$

221 where $z' = (z - z_{\text{top}})/(z_{\text{base}} - z_{\text{top}})$ denotes the fractional
222 cloud height with $z' = 0$ for the cloud top and $z' = 1$ for the
223 cloud base. Thus, the linear r_e profile is parameterized by r_{e1}
224 at $z' = 0$ and r_{e2} at $z' = 1$ representing the cloud top and
225 cloud base r_e , respectively. The retrievals of r_{e1} and r_{e2} are
226 determined by matching the MODIS measurements with
227 radiative transfer calculations at 3.7 , 2.1 , and $1.6 \mu\text{m}$.
228 Chang and Li [2002] analyzed the potential biases
229 associated with the assumption of a linear r_e profile and
230 those arising from reflectance error. They showed that the
231 linear r_e profile retrieval works best for cloud optical depths
232 ranging between 10 and 28. The retrieval mean biases are
233 on the order of $1 \mu\text{m}$ for cloud top and slightly larger for
234 cloud base if the r_e profile has a close-to-linear variation.
235 However, if the r_e variation is very nonlinear, large biases
236 may be incurred, in particular for cloud base r_e . Also when
237 clouds have large optical depth (>28), the quality of r_e
238 profile estimation does not change much for cloud top but

gets much worse for cloud base because the signal from 239
cloud base is weak for thick clouds. Over all, the uncertainties 240
in r_{e2} are typically 2–3 times larger than the uncertainties in 241
 r_{e1} . 242

[13] Traditionally, with the assumption that r_e is vertically 243
constant, cloud LWP is derived as given by 244

$$LWP = \frac{4\rho_w}{3Q_e} \tau r_e, \quad (2)$$

Here, τ is the cloud optical depth, ρ_w is the density of liquid 246
water, $Q_e (=2)$ is the extinction efficiency. Previously, r_e 247
retrieved with reflectance measurements using a single NIR 248
channel have been used to calculate LWP with equation (2). 249
As discussed earlier, the r_e retrieved from a single NIR 250
channel like $3.7 \mu\text{m}$ is more sensitive to the layer near the 251
cloud top, which can cause biases in LWP calculations for 252
cloud with vertical r_e variation. In the CL algorithm, cloud 253
optical depth is retrieved from MODIS $0.86\text{-}\mu\text{m}$ reflectance 254
measurement for clouds over ocean and LWP is calculated 255
with the linear r_e profile estimation. Chen *et al.* [2007] 256
showed that MODIS LWP estimation using CL algorithm is 257
consistent with LWP retrieved from AMSR-E microwave 258
observations (i.e., correlation coefficient is around 0.9 for 259
overcast clouds with warm top) and LWP calculation with r_e 260
profile corrects the biases caused by the assumption of 261
vertically constant r_e . 262

263 2.4. Spatial and Temporal Matching of MODIS and 264 C-Band Data

[14] For each RHB location covered by a MODIS scan 265
(a total of five MODIS overpasses during the 6 d during 266
EPIC), the r_e profile retrievals are compared with coincident 267
RHB scanning C-band radar measurements. MODIS pro- 268
vides instantaneous measurements, while the temporal res- 269
olution of the C-band radar is 5 min. To alleviate the 270
influence of the small, but nonnegligible, temporal gap 271
between the two instruments, both MODIS data and C-band 272
data are aggregated and averaged within $5 \times 5 \text{ km}$ boxes. 273
We aggressively discard aggregated samples that are not 274
fully overcast by insisting that all 25 pixels must contain 275
cloud. There are large uncertainties and ambiguities in 276
retrieval of effective radius if the clouds are very thin 277
(i.e., optical thickness is less than 4) [Nakajima and King, 278
1990]. In this study, to ensure reliable retrieval of cloud 279
parameters, the optical depths for all cloudy pixels are 280
required to be larger than 4. These constraints have been 281
applied to ensure that as many broken, thin, and highly 282
heterogeneous MODIS pixels (i.e., those most likely to 283
violate the plane-parallel retrieval assumption) are not 284
included in the analysis. 285

[15] The C-band radar measurements are compared with 286
the r_e profile retrieval from MODIS on board Terra satellite. 287
As an example of these data, Figure 2 shows coincident 288
images of C-band radar reflectivity, MODIS r_e profile 289
retrieval (i.e., r_{e1} and r_{e2}) and MODIS LWP estimates at 290
1555 UTC of 18 October 2001, a period of strong drizzle 291
also shown in the MMCR data (Figure 1). Data in which 292
cloud is not present or broken, as detailed above, are 293
blanked out. There is considerable heterogeneity in the 294
precipitation field but it is clear that regions of strong 295
drizzle (large Z) are generally associated with higher LWP 296

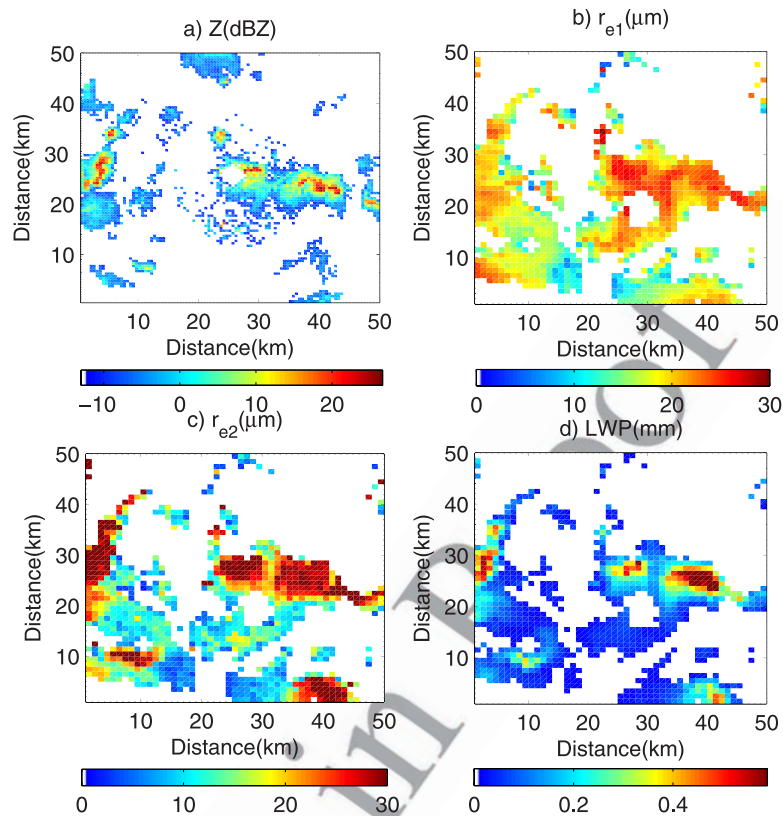


Figure 2. Coincident images of C-band radar reflectivity and MODIS cloud profile at UTC 1555, 18 October 2001. (a) RHB C-band radar reflectivity image. (b) MODIS estimation of droplet effective radius at cloud top (r_{e1}). (c) MODIS estimation of droplet effective radius at cloud base (r_{e2}). (d) MODIS LWP estimation.

297 and large drops at cloud base (i.e., large r_{e2}). There is also a
 298 correlation of Z with the cloud top effective radius r_{e1} but it
 299 is not as clear as with r_{e2} . This is consistent with the idea
 300 that, for heavy drizzle, the drizzle drops themselves may be
 301 directly impacting the drop effective radius close to the
 302 cloud base. We return to this issue in section 3.2.

304 3. Results

305 3.1. MMCR Reflectivity Profile and Estimates of the 306 Partitioning of Liquid Water Content Between Drizzle 307 Drops and Small Cloud Droplets

308 [16] Figure 3 shows the scatterplot of mean radar reflectivity Z
 309 over the upper third ($0 < z' < 1/3$) and lower third ($2/3 < z' < 1$)
 310 of the cloud layer, with z' determined using the cloud top and
 311 base heights from the MMCR and ceilometer, respectively. The
 312 column maximum reflectivity is shown by the color of the data
 313 samples. Radar reflectivity Z depends on the sixth moment of
 314 the cloud and drizzle size distribution. Radar reflectivity
 315 thresholds for drizzle detection generally range between -20 dBZ
 316 and -15 dBZ in previous studies [Sauvageot and Omar, 1987;
 317 Wang and Geerts, 2003; Kogan et al., 2005]. For drizzling
 318 clouds, the reflectivity due to precipitation drops starts to
 319 overwhelm that due to cloud droplets and corresponds to precipi-
 320 tation rates of only a few thousandths of a mm hr^{-1} . Thus even
 321 modest amounts of precipitation can overwhelm the radar signal
 322 due to cloud droplets [Fox and Illingworth, 1997] even

when the drizzle has limited effect on the overall liquid
 324 water content and effective radius of the cloud. Figure 3
 325 shows that cloud top Z is greater than cloud base Z for
 326 nondrizzling clouds (i.e., column maximum reflectivity is 327

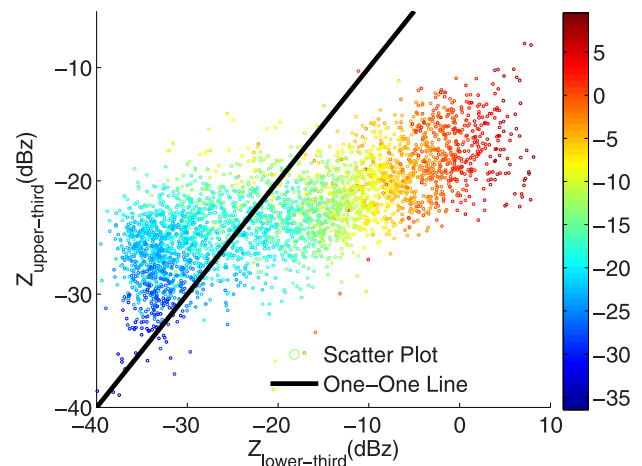


Figure 3. Scatterplot of reflectivities over upper 1/3 portion of cloud layer ($Z_{\text{upper-third}}$) and reflectivities over lower 1/3 portion of cloud layer ($Z_{\text{lower-third}}$). Color of the scatterplots represents the column maximum radar reflectivity. The data is from MMCR.

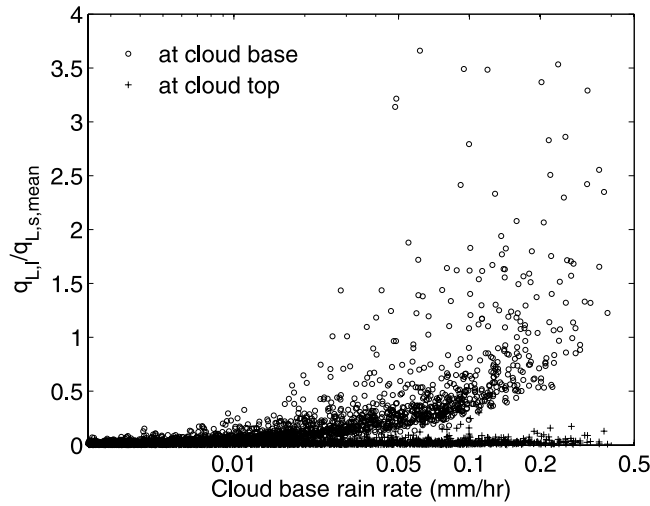


Figure 4. Scatterplot of the ratio between the liquid water content of drizzle drops ($q_{L,l}$) and the column mean liquid water content of small droplets ($q_{L,s,mean}$) versus rain rate at cloud base. Circles represent $q_{L,l,base}/q_{L,s,mean}$ at cloud base and pluses represent $q_{L,l,top}/q_{L,s,mean}$ at cloud top. The estimates are made with data from shipborne MMCR and microwave radiometer.

328 -30 dBZ), while the opposite is true for drizzling clouds
 329 (i.e., column maximum reflectivity is -10 dBZ) (a result
 330 consistent with *Comstock et al.* [2004, Figure 4]). For
 331 nondrizzling clouds, cloud droplet size and number con-
 332 centration determines Z , and its increase with height is
 333 caused primarily by condensational growth of cloud drop-
 334 lets. Drizzle drops dominate radar reflectivity in drizzling
 335 clouds. Aircraft observations [*Wood*, 2005a] show that in
 336 drizzling stratocumulus the precipitation rate tends to be
 337 roughly constant in the lowest two thirds of the cloud layer
 338 before decreasing rapidly above this. For drizzling clouds in
 339 Figure 3, the large reflectivity in the lower portion of the
 340 cloud layer is caused by drizzle at cloud base, while the
 341 small radar reflectivity at upper portion of cloud layer is
 342 consistent with there being much less drizzle near cloud top.
 343 [17] *Wood* [2000] found that drizzle drops start to increase
 344 effective radius significantly if $\phi = q_{L,l}/q_{L,s}$ is above 0.1,
 345 where $q_{L,l}$ is the liquid water content of large drops ($r >$
 346 $20 \mu\text{m}$) and $q_{L,s}$ is the liquid water content of small ($r <$
 347 $20 \mu\text{m}$) cloud droplets. His study found that it is possible
 348 to parameterize the impact of drizzle drops on effective
 349 radius as

$$\frac{r_e}{r_{e,s}} \approx \frac{(1 + \phi)^{\frac{2}{3}}}{\left\{ 1 + 0.2 \left(\frac{k_l}{k_s} \right)^{\frac{1}{3}} \phi \right\}} \quad (3)$$

351 where r_e is the effective radius for all droplets, $r_{e,s}$ is the
 352 effective radius for small cloud droplets, k_l is the ratio
 353 between the cubes of the volume and effective radius for
 354 large drops, and k_s is the ratio between the cubes of the
 355 volume and effective radius for small droplets. In his study,
 356 k_l is parameterized as $2/9$ (the exact value for an exponential
 357 distribution to which populations of drizzle drops adhere
 358 quite closely [*Wood*, 2005b]) and k_s ranges between

approximately 0.6 and 0.9 [e.g., *Martin et al.*, 1994]. On 359
 the basis of equation (3), with the assumption of k_s equal to 360
 0.75, the drizzle drops would increase r_e by 40% for $\phi = 1$ 361
 and 10% for $\phi = 0.2$. With the MMCR reflectivity profile 362
 and the LWP estimation from RHB microwave radiometer, 363
 liquid water content of drizzle drops and liquid water 364
 content of small cloud droplets can be roughly estimated. 365
 The liquid water content of drizzle drops at cloud base is 366
 estimated with $q_{L,l} = \rho R/w_T$, where R is cloud base 367
 precipitation rate, ρ is the density of water, and w_T is the 368
 mass-weighted fall speed of drizzle drops. Using a typical 369
 fall speed of 0.4 m s^{-1} for drizzle drops (consistent with the 370
 aircraft data of *Wood* [2005a] for which w_T is in the range 371
 $0.2-0.6 \text{ m s}^{-1}$), the drizzle liquid water content would be 372
 $q_{L,l} \approx 0.69R$ in g m^{-3} . The rain rate profile can be estimated 373
 from the MMCR reflectivity profile with $Z = 25 R^{1.3}$ 374
 [*Comstock et al.*, 2004]. Thus, the LWP contributed by 375
 drizzle drops (LWP_l) is the vertical integral of $0.69R$ over 376
 the depth of the precipitating layer, and LWP contributed by 377
 small cloud droplets (LWP_s) is estimated by subtracting 378
 LWP_l from total LWP estimated with RHB microwave 379
 radiometer measurements. The mean liquid water content of 380
 small droplets ($q_{L,s,mean}$) can be estimated from the mean 381
 LWP_s over the cloud depth. Figure 4 shows estimated 382
 $q_{L,l,base}/q_{L,s,mean}$ and $q_{L,l,top}/q_{L,s,mean}$ against R_{cb} , where 383
 $q_{L,l,base}$ is the liquid water content of drizzle drops at cloud 384
 base, $q_{L,l,top}$ is the liquid water content of drizzle drops at 385
 cloud top, and R_{cb} is the rain rate at cloud base. It is shown 386
 that the $q_{L,l,base}/q_{L,s,mean}$ grows from <0.1 at $R_{cb} < 0.01 \text{ mm}$ 387
 h^{-1} to >1 as R_{cb} reaches a few tenths of a mm h^{-1} , while 388
 $q_{L,l,top}$ is always much smaller than $q_{L,s,mean}$. Because the 389
 radius of small cloud droplets generally increases with 390
 height, $q_{L,s}$ at cloud base is expected to be less than $q_{L,s,mean}$ 391
 and $q_{L,l}/q_{L,s}$ at cloud base is expected to be larger than 392
 $q_{L,l,base}/q_{L,s,mean}$ and so the ratios of drizzle to cloud liquid 393
 water presented in Figure 4 are representative of the cloud 394
 as a whole and most likely underestimate the impact of 395
 drizzle close to cloud base. In any case, taken together with 396
 equation (3), such ratios are consistent with drizzle having 397
 an impact on the effective radius when the precipitation rate 398
 exceeds a few hundredths of a mm h^{-1} . It is remarkable that 399
 for even relatively modest precipitation rates, a significant 400
 fraction of the liquid water content in stratocumulus clouds 401
 can reside in drizzle-sized drops. The impacts of drizzle 402
 upon r_e at cloud base could significantly change the trend of 403
 vertical r_e variation because there are not many drizzle 404
 drops at cloud top. Using the r_e profile estimated from 405
 satellite reflectance measurements, the following section 406
 assesses the impact of drizzle drops on vertical r_e variation 407
 in detail. 408

3.2. Satellite Estimates of the r_e Profile for Drizzling and Nondrizzling Clouds

[18] Figure 5 shows the C-band precipitation rate against 411
 the MODIS-derived droplet effective radius at cloud top r_{e1} 412
 and cloud base r_{e2} for the spatially matched data set from 413
 EPIC. A threshold of -12 dBZ (minimum detectable 414
 reflectivity of the C-band radar) is used to classify the $5 \times$ 415
 5 km regions into either drizzling or nondrizzling. Statistics 416
 of r_{e1} and r_{e2} are shown in Table 1. Both r_{e1} and r_{e2} are 417
 larger for drizzling clouds than for nondrizzling clouds, with 418
 a threshold for drizzle of approximately $15 \mu\text{m}$ in r_{e1} 419

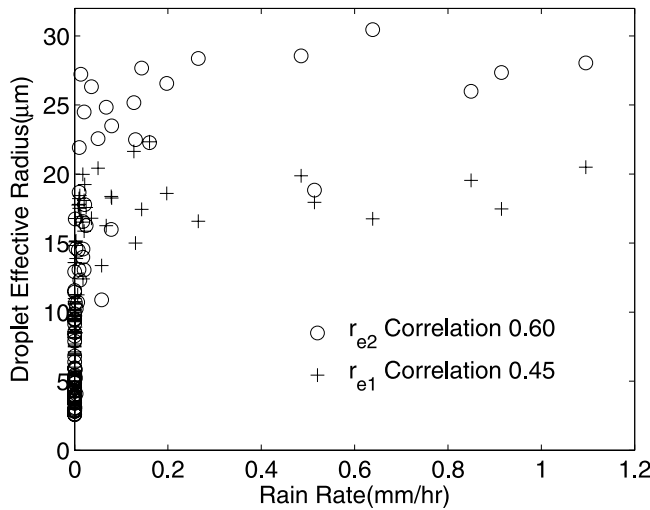


Figure 5. Scatterplot between rain rates and cloud droplet effective radius. Here r_{e1} is droplet effective radius at cloud top and r_{e2} is droplet effective radius at cloud base. The estimates are made with data from MODIS and C-band radar.

consistent with earlier in situ studies [e.g., Gerber, 1996]. However, r_{e2} shows a greater contrast between drizzling clouds and nondrizzling clouds. The mean value of r_{e1} is $9.6 \mu\text{m}$ for nondrizzling cloud and $17.1 \mu\text{m}$ for drizzling clouds, while the mean value of r_{e2} is $6.3 \mu\text{m}$ for nondrizzling cloud and $20.8 \mu\text{m}$ for drizzling clouds. The correlation coefficient with rain rate is 0.45 for r_{e1} and is 0.60 for r_{e2} . The reason that r_{e2} is better correlated with rain rate is that the drizzle drops at cloud base increase the effective radius. On the other hand, drizzle decreases markedly toward the cloud top. The correlation between precipitation rate and cloud top effective radius is therefore expected not because the precipitation itself contributes to r_e but because clouds with large drops near their tops will be more prone to collision-coalescence which ultimately manifests itself as greater precipitation rates lower down in the cloud.

[19] Figure 6 shows the scatterplot between r_{e1}/r_{e2} and coincident rain rate. Values of r_{e1} are generally larger than r_{e2} for nondrizzling clouds and the mean value of r_{e1}/r_{e2} is 1.61 for nondrizzling clouds. The ratio decreases as the clouds start to drizzle and can become less than unity if drizzle is heavy (i.e., larger than 0.2 mm h^{-1}). The mean rain rate is 0.04 mm h^{-1} for drizzling clouds with $r_{e1}/r_{e2} > 1$ and 0.18 mm h^{-1} for drizzling clouds with $r_{e1}/r_{e2} < 1$. The mean value of r_{e1}/r_{e2} is 0.92 for drizzling cloud. The correlation coefficient between r_{e1}/r_{e2} and rain rate is -0.43 .

[20] Using rain rate estimation from the C-band radar and LWP from MODIS, we can make a rough estimate of $q_{L,1}/q_{L,s}$ using the same method as in section 3.1. Figure 7

shows a plot of the precipitation rate against LWP. For drizzling cloud, the mean rain rate is 0.15 mm h^{-1} and the mean cloud LWP is 0.16 mm . As discussed in section 3.1, the drizzle liquid water content would be $0.69R$ in g m^{-3} . The 0.15 mm h^{-1} mean rain rate in Figure 7 means a drizzle liquid water content of $q_{L,1}$ of $\sim 0.10 \text{ g m}^{-3}$. The average thickness of a drizzling cloud is around 0.6 km for the data used in this study (estimated with MMCR and ceilometer). For an average cloud LWP of 0.16 mm in Figure 7, the average cloud liquid water content ($q_{L,1} + q_{L,s}$) is around 0.25 g m^{-3} and $q_{L,s}$ would be around 0.15 g m^{-3} after the 0.10 g m^{-3} $q_{L,1}$ is subtracted. Considering that $q_{L,s}$ at cloud base is less than $q_{L,s}$ at cloud top because r_{e1}/r_{e2} is larger than 1 without contribution from drizzle drops, $q_{L,s}$ would be in the same order of magnitude as $q_{L,1}$ at cloud base for the average rain rate of 0.15 mm h^{-1} . Certainly, $q_{L,1}$ would be smaller than $q_{L,s}$ when the drizzle is light (i.e., 0.01 mm h^{-1}) and would be larger than $q_{L,s}$ when the drizzle is high (i.e., 0.5 mm h^{-1}).

[21] The above comparison of $q_{L,1}$ with $q_{L,s}$ indicates that, for the drizzling clouds in Figure 6, we expect a significant amount of drizzle liquid water content close to cloud base, especially when the precipitation rate exceeds about 0.1 mm h^{-1} . Given that the drizzle drops start to increase effective radius significantly if $q_{L,1}/q_{L,s}$ is above 0.1, the neutralization and conversion of the trends of r_e vertical variation by drizzle drops in Figure 6 is consistent with theoretical calculations by Wood [2000] and with in situ observations [Martin et al., 1994].

[22] Chen et al. [2007] also suggested similar impact of drizzle on vertical r_e variation, but in that preliminary study the r_e decreases with height for most precipitating clouds, and could be either increasing or decreasing for nonprecipitating clouds. As previously stated, this investigation found that most nondrizzling clouds have a r_e profile that increases with height and drizzling clouds have r_e profiles that either increase or decrease with height. The differences between the results of the two studies are caused by utilizing different drizzle detection techniques. As stated in section 1, AMSR-E rain detection used in the work of Chen et al. [2007] misses light drizzle and possibly some heavy drizzle if the cloud LWP is low. As a result, the drizzle defined by AMSR-E is necessarily heavy drizzle, while the nondrizzling clouds defined by AMSR-E contain both drizzling and nondrizzling clouds.

4. Summary and Future Studies

[23] Using data from the EPIC 2001 Stratocumulus Study, this study investigates the cloud r_e vertical variation for drizzling and nondrizzling clouds. Estimates of the partitioning of liquid water content between drizzle drops and small cloud droplets is carried out using MMCR data in drizzling stratocumulus by incorporating simultaneous LWP

t1.1 **Table 1.** Comparison of Cloud Parameters for Raining Clouds and Nonraining Clouds

t1.2	$r_{e1}(\mu\text{m})$	$r_{e2}(\mu\text{m})$	r_{e1}/r_{e2}	Cloud LWP (mm)	Rain Rate (mm h^{-1})	
t1.3	Correlation with rain rate	0.45	0.60	-0.44	0.76	N/A
t1.4	Mean for nonraining clouds	9.6	6.3	1.61	0.034	0
t1.5	Mean for raining clouds	17.1	20.8	0.92	0.155	0.149

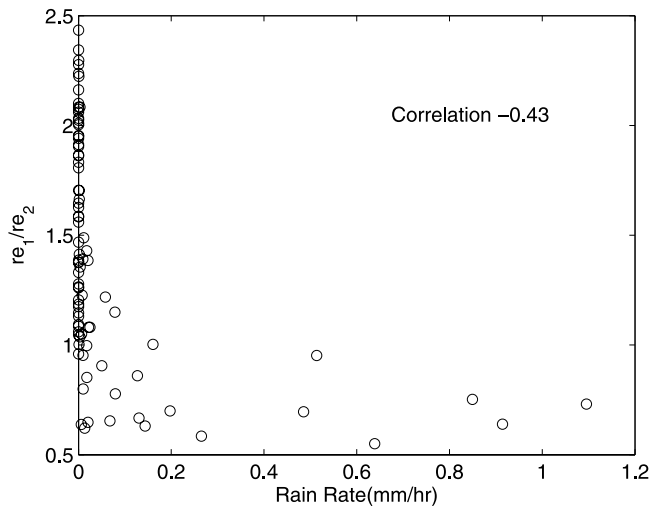


Figure 6. Scatterplot between rain rates and ratio between droplet effective radius at cloud top (r_{e1}) and droplet effective radius at cloud base (r_{e2}). The estimates are made with data from MODIS and C-band radar.

502 estimates from a passive microwave radiometer. Satellite
 503 reflectance measurements from MODIS on the Terra satel-
 504 lite are used to estimate the trend of vertical r_e variation.
 505 Using drizzle rates estimated with a scanning C-band radar
 506 we show that the cloud r_e can decrease with height in clouds
 507 with sufficiently strong drizzle. For nondrizzling clouds, the
 508 r_e generally increases with height in accordance with the
 509 growth of cloud droplets by condensation. For drizzling
 510 clouds, at cloud base, liquid water content of drizzle drops is
 511 found to be of comparable magnitude to liquid water
 512 content of small cloud droplets when rain rate at cloud base
 513 is above a few hundredths of a mm h^{-1} . Both previous
 514 theoretical analyses [Wood, 2000] and the synergetic obser-
 515 vations in this study suggest that drizzle drops can increase
 516 r_e significantly at drizzle rates found in low liquid water
 517 clouds. Because drizzle is typically found toward the
 518 bottom of these clouds, the r_e increase by drizzle drops at
 519 cloud base can change the trend of vertical r_e variation and
 520 r_e can decrease with height if drizzle is heavy. On the basis
 521 of the radar precipitation observations and satellite cloud r_e
 522 profile estimation, r_e generally decreases with height when
 523 rain rate is above 0.1 mm h^{-1} .

524 [24] Both r_e at cloud base and r_e at cloud top are shown to
 525 have certain distinction between drizzling and nondrizzling
 526 clouds: larger for drizzling clouds than for nondrizzling
 527 clouds. The distinction is more striking for r_e at cloud base
 528 than r_e at cloud top. The r_e at cloud base is also found to be
 529 better correlated with rain rate. The finding of this study
 530 suggests that the profile of r_e or r_e at cloud base has the
 531 potential for drizzle detection in marine low clouds. Drizzle
 532 detection is very important in climate studies because
 533 drizzle can affect the optical properties of low clouds by
 534 changing their macrophysical and microphysical structure
 535 [e.g., Albrecht, 1989; Stevens et al., 2005; Wood, 2007]. It is
 536 important to develop methodologies for the detection and
 537 quantification of drizzle and other light precipitation in low
 538 clouds.

[25] Both space-borne passive microwave observations 539
 and solar observations have been used for detection of 540
 drizzle. Drizzle detection with passive microwave observa- 541
 tion uses the estimation of column LWP, which contains 542
 both cloud liquid water and drizzle liquid water. The 543
 threshold of LWP for drizzle detection is about 0.2 mm 544
 [Ferraro et al., 1996; Wentz and Spencer, 1998]. Micro- 545
 wave observation has the advantage of being sensitive to 546
 drizzle directly, but the ambiguity caused by cloud liquid 547
 water may degrade its performance in detection of light 548
 drizzle. Zuidema et al. [2005] found that light drizzle is 549
 common even at low LWP. Depending upon the microphys- 550
 ical cloud properties such as cloud droplet concentration the 551
 column LWP can be very small (i.e., 0.05 mm) for light 552
 drizzle with small rain rate (e.g., 0.02 mm h^{-1} [Wood, 553
 2005a]). On the other hand, the cloud LWP can be as large 554
 as $0.2\text{--}0.4 \text{ mm}$ even for nondrizzling clouds [Wood, 2005a; 555
 Berg et al., 2006]. If a 0.2 mm threshold of column LWP is 556
 applied for drizzle detection, most light drizzle with rain 557
 rate less than 0.1 mm h^{-1} would be missed. Given that 558
 typical precipitation rates in marine low clouds range from 559
 0.01 to 0.1 mm h^{-1} [e.g., Yum and Hudson, 2002; Wood, 560
 2005a], this detection threshold will miss a significant 561
 fraction of drizzling clouds over the oceans. Indeed, results 562
 from EPIC show that for these clouds approximately 80% of 563
 the drizzling area consists of precipitation rates smaller than 564
 0.1 mm h^{-1} and that these weakly drizzling clouds contrib- 565
 ute around 25% of the accumulated precipitation at cloud 566
 base [Comstock et al., 2004, Figure 9]. 567

[26] Drizzle detection with solar reflectance observations 568
 has used cloud r_e retrieved from single NIR channels. The r_e 569
 threshold for drizzle detection is about $14 \mu\text{m}$ in previous 570
 studies [Rosenfeld and Gutman, 1994; Han et al., 1995]. 571
 However, the r_e retrieved from a single NIR channel is 572
 biased toward cloud top, whereas most drizzle is found 573
 lower down in the cloud. For example, r_e retrieval from 574
 $3.7 \mu\text{m}$ represent most top of the cloud layer, while r_e 575
 retrieved from $2.1 \mu\text{m}$ may represent upper 20% \sim 40% 576
 optical depth of cloud layer with optical depth equal 577
 8 [Nakajima and King, 1990]. As previously stated, be- 578
 tween drizzling clouds and nondrizzling clouds, there is a 579

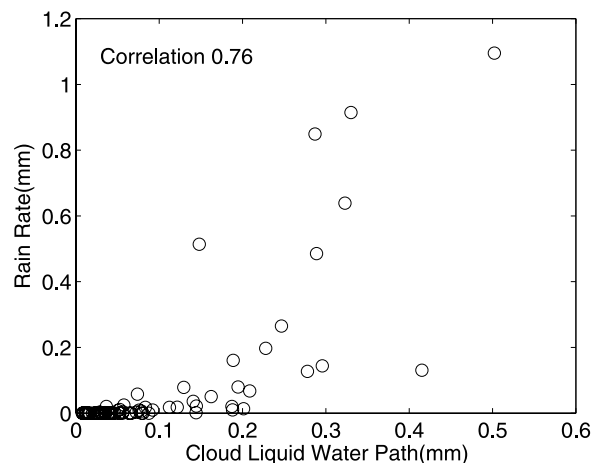


Figure 7. Scatterplot between rain rates and liquid water paths. The estimates are made with data from MODIS and C-band radar.

580 difference in r_e at cloud top, but a greater contrast in r_e at
 581 cloud base due to the drizzle drops at cloud base for
 582 drizzling clouds.

583 [27] Results of this study shows that satellite r_e profile
 584 estimation (r_{e2} at cloud base or ratio r_{e1}/r_{e2}) could be used as
 585 another method for drizzle detection in marine low clouds.
 586 The technique details and the quality of the methods beyond
 587 the scope of this study because limited data has been
 588 available. Future study on this topic could be done when
 589 CloudSat data and more campaign data are available.

590 [28] **Acknowledgments.** EPIC 2001 was a cooperative effort among
 591 many scientists, students, staff, and the crew and officers of the R/V *Ronald*
 592 *H. Brown*. The authors appreciate their work of acquiring the EPIC 2001
 593 data used in this study. The authors are grateful to the Goddard DAAC for
 594 providing MODIS LIB data. This study is supported by the NOAA's
 595 GOES-R risk reduction program, the GOES-R algorithm development
 596 program, and a grant from the National Science Foundation (ATM
 597 0433712).

598 References

- 599 Albrecht, B. A. (1989), Aerosols, cloud microphysics and fractional cloudi-
 600 ness, *Science*, *245*, 1227–1230, doi:10.1126/science.245.4923.1227.
- 601 Ashcroft, P., and F. J. Wentz (2000), AMSR algorithm theoretical basis
 602 document, *Tech. Rep. 121599B-1*, 27 pp., Remote Sensing Syst., Santa
 603 Rosa, Calif.
- 604 Berg, W., T. L'Ecuyer, and C. Kummerow (2006), Rainfall climate regimes:
 605 The relationship of regional TRMM rainfall biases to the environment,
 606 *J. Appl. Meteorol. Climatol.*, *45*, 434–454, doi:10.1175/JAM2331.1.
- 607 Brenguier, J. L., H. Pawlowska, L. Schüller, R. Preusker, J. Fischer, and
 608 Y. Fouquart (2000), Radiative properties of boundary layer clouds: Dro-
 609 plet effective radius versus number concentration, *J. Atmos. Sci.*, *57*,
 610 803–821, doi:10.1175/1520-0469(2000)057<0803:RPOBLC>2.0.CO;2.
- 611 Bretherton, C. S., T. Uttal, C. W. Fairall, S. E. Yuter, R. A. Weller,
 612 D. Baumgardner, K. Comstock, and R. Wood (2004), The EPIC
 613 2001 stratocumulus study, *Bull. Am. Meteorol. Soc.*, *85*, 967–977,
 614 doi:10.1175/BAMS-85-7-967.
- 615 Chang, F.-L., and Z. Li (2002), Estimating the vertical variation of
 616 cloud droplet effective radius using multispectral near-infrared satellite
 617 measurements, *J. Geophys. Res.*, *107*(D7), 4257, doi:10.1029/
 618 2001JD000766.
- 619 Chang, F.-L., and Z. Li (2003), Retrieving vertical profiles of water-cloud
 620 droplet effective radius: Algorithm modification and preliminary applica-
 621 tion, *J. Geophys. Res.*, *108*(D3), 4763, doi:10.1029/2003JD003906.
- 622 Chen, R., F.-L. Chang, Z. Li, R. Ferraro, and F. Weng (2007), Impact of the
 623 vertical variation of cloud droplet size on the estimation of cloud liquid
 624 water path and rain detection, *J. Atmos. Sci.*, *64*, 3843–3853.
- 625 Comstock, K. K., R. Wood, S. E. Yuter, and C. S. Bretherton (2004),
 626 Reflectivity and rain rate in and below drizzling stratocumulus, *Q.J.R.*
 627 *Meteorol. Soc.*, *130*, 2891–2918, doi:10.1256/qj.03.187.
- 628 Ferraro, R. R., N. C. Grody, F. Weng, and A. Basist (1996), An eight-year
 629 (1987–1994) time series of rainfall, clouds, water vapor, snow cover, and
 630 sea ice derived from SSM/I measurements, *Bull. Am. Meteorol. Soc.*, *77*,
 631 891–906, doi:10.1175/1520-0477(1996)077<0891:AEYTSO>2.0.CO;2.
- 632 Fox, N. I., and A. J. Illingworth (1997), The retrieval of stratocumulus
 633 cloud properties by ground-based cloud radar, *J. Appl. Meteorol.*, *36*,
 634 485–492, doi:10.1175/1520-0450(1997)036<0485:TROSCP>2.0.CO;2.
- 635 Gerber, H. (1996), Microphysics of marine stratocumulus clouds with two
 636 drizzle modes, *J. Atmos. Sci.*, *53*(12), 1649–1662, doi:10.1175/1520-
 637 0469(1996)053<1649:MOMSCW>2.0.CO;2.
- 638 Greenwald, T. J., G. L. Stephens, S. A. Christopher, H. Vonder, and
 639 H. Thomas (1995), Observations of the global characteristics and regional
 640 radiative effects of marine cloud liquid water, *J. Clim.*, *8*, 2928–2946,
 641 doi:10.1175/1520-0442(1995)008<2928:OOTGCA>2.0.CO;2.
- 642 Han, Q., W. B. Rossow, and A. A. Lacis (1994), Near-global survey of
 643 effective droplet radii in liquid water clouds using ISCCP data, *J. Clim.*,
 644 *7*, 465–497, doi:10.1175/1520-0442(1994)007<0465:NGSOED>2.0.
 645 CO;2.
- 646 Han, Q., W. B. Rossow, R. Welch, A. White, and J. Chou (1995), Validation
 647 of satellite retrievals of cloud microphysics and liquid water path using
 648 observation from FIRE, *J. Atmos. Sci.*, *52*, 4183–4195, doi:10.1175/
 649 1520-0469(1995)052<4183:VOSROC>2.0.CO;2.
- 650 King, M. D., W. P. Menzel, Y. J. Kaufman, D. Tanre, B. C. Gao, S. Platnick,
 651 S. A. Ackerman, L. A. Remer, R. Pincus, and P. A. Hubanks (2003),
 Cloud and aerosol properties, precipitable water, and profiles of tempera-
 652 ture and humidity from MODIS, *IEEE Trans. Geosci. Remote Sens.*, *41*,
 653 442–458, doi:10.1109/TGRS.2002.808226.
- 654 Klein, S. A., and D. L. Hartmann (1993), The seasonal cycle of low strati-
 655 form clouds, *J. Clim.*, *6*, 1587–1606, doi:10.1175/1520-0442(1993)
 656 006<1587:TSCOLS>2.0.CO;2.
- 657 Kobayashi, T. (2007), Significant differences in the cloud droplet effective
 658 radius between nonprecipitating and precipitating clouds, *Geophys. Res.*
 659 *Let.*, *34*, L15811, doi:10.1029/2007GL029606.
- 660 Kogan, Z. N., D. B. Mechem, and Y. L. Kogan (2005), Assessment of
 661 variability in continental low stratiform clouds based on observations
 662 of radar reflectivity, *J. Geophys. Res.*, *110*, D18205, doi:10.1029/
 663 2005JD006158.
- 664 Martin, G. M., D. W. Johnson, and A. Spice (1994), The measurement and
 665 parameterization of effective radius of droplets in warm stratocumulus
 666 clouds, *J. Atmos. Sci.*, *51*, 1823–1842, doi:10.1175/1520-0469(1994)
 667 051<1823:TMAPOE>2.0.CO;2.
- 668 Miles, N. L., J. Verlinde, and E. E. Clothiaux (2000), Cloud droplet size
 669 distributions in lowlevel stratiform clouds, *J. Atmos. Sci.*, *57*, 295–311,
 670 doi:10.1175/1520-0469(2000)057<0295:CDSJIL>2.0.CO;2.
- 671 Moran, K. P., B. E. Martner, M. J. Post, R. A. Kropfli, D. C. Welsh, and
 672 K. B. Widener (1998), An unattended cloud-profiling radar for use in
 673 climate research, *Bull. Am. Meteorol. Soc.*, *79*, 443–455, doi:10.1175/
 674 1520-0477(1998)079<0443:AUCPRF>2.0.CO;2.
- 675 Nakajima, T., and M. D. King (1990), Determination of the optical thick-
 676 ness and effective particle radius of clouds from the reflected solar radia-
 677 tion measurements. Part I: Theory, *J. Atmos. Sci.*, *47*(15), 1878–1893,
 678 doi:10.1175/1520-0469(1990)047<1878:DOTOTA>2.0.CO;2.
- 679 Platnick, S. (2000), Vertical photon transport in cloud remote sensing prob-
 680 lems, *J. Geophys. Res.*, *105*, 22,919–22,935, doi:10.1029/
 681 2000JD900333.
- 682 Rosenfeld, D., and G. Gutman (1994), Retrieving microphysical properties
 683 near the tops of potential rain clouds by multispectral analysis of AVHRR
 684 data, *Atmos. Res.*, *34*, 259–283, doi:10.1016/0169-8095(94)90096-5.
- 685 Sauvageot, H., and J. Omar (1987), Radar reflectivity of cumulus clouds,
 686 *J. Atmos. Oceanic Technol.*, *4*, 264–272, doi:10.1175/1520-0426
 687 (1987)004<0264:RROCC>2.0.CO;2.
- 688 Stevens, B., G. Vali, K. Comstock, R. Wood, M. C. van Zanten, P. H.
 689 Austin, C. S. Bretherton, and D. H. Lenschow (2005), Pockets of open
 690 cells and drizzle in marine stratocumulus, *Bull. Am. Meteorol. Soc.*, *86*,
 691 51–57, doi:10.1175/BAMS-86-1-51.
- 692 VanZanten, M. C., B. Stevens, G. Vali, and D. H. Lenschow (2005), Ob-
 693 servations of drizzle in nocturnal marine stratocumulus, *J. Atmos. Sci.*,
 694 *62*, 88–106, doi:10.1175/JAS-3355.1.
- 695 Wang, J., and B. Geerts (2003), Identifying drizzle within marine stratus
 696 with W-band radar reflectivity, *Atmos. Res.*, *69*, 1–27, doi:10.1016/j.
 697 atmosres.2003.08.001.
- 698 Wentz, F. J., and R. W. Spencer (1998), SSM/I rain retrievals within a
 699 unified all-weather ocean algorithm, *J. Atmos. Sci.*, *55*, 1613–1627,
 700 doi:10.1175/1520-0469(1998)055<1613:SIRRAW>2.0.CO;2.
- 701 Wood, R. (2000), Parameterization of the effect of drizzle upon the droplets
 702 effective radius in stratocumulus clouds, *Q.J.R. Meteorol. Soc.*, *126*,
 703 3309–3324, doi:10.1002/qj.49712657015.
- 704 Wood, R. (2005a), Drizzle in stratiform boundary layer clouds. Part I:
 705 Vertical and horizontal structure, *J. Atmos. Sci.*, *62*, 3011–3033,
 706 doi:10.1175/JAS3529.1.
- 707 Wood, R. (2005b), Drizzle in stratiform boundary layer clouds. Part II:
 708 Microphysical aspects, *J. Atmos. Sci.*, *62*, 3034–3050, doi:10.1175/
 709 JAS3530.1.
- 710 Wood, R. (2007), Cancellation of aerosol indirect effects in marine strato-
 711 cumulus through cloud thinning, *J. Atmos. Sci.*, *64*, 2657–2669,
 712 doi:10.1175/JAS3942.1.
- 713 Yum, S. S., and J. G. Hudson (2002), Maritime/continental microphysical
 714 contrasts in stratus, *Tellus, Ser. B*, *54*, 61–73.
- 715 Zuidema, P., E. R. Westwater, C. Fairall, and D. Hazen (2005), Ship-based
 716 liquid water path estimates in marine stratocumulus, *J. Geophys. Res.*,
 717 *110*, fD20206, doi:10.1029/2005JD005833.

F.-L. Chang, National Institute for Aerospace, Hampton, VA 23666,
 720 USA.

R. Chen and Z. Li, Department of Atmospheric and Oceanic Sciences,
 722 University of Maryland, College Park, MD 20742, USA. (zli@atmos.
 723 umd.edu)

R. Ferraro, Cooperative Institute for Climate Studies, University of
 725 Maryland, College Park, MD 20742, USA.

R. Wood, Department of Atmospheric Sciences, University of Washington,
 727 Seattle, WA 98195, USA.